

Five-fold Symmetry in Au-Si Metallic Glass

Chang-Chun He,^{†,‡} Shao-Gang Xu,[†] Shao-Bin Qiu,[‡] Chao He,[†] Yu-Jun Zhao,[‡]
 Xiao-Bao Yang,^{*,‡,¶} and Hu Xu^{*,†,¶}

[†]*Department of Physics, Southern University of Science and Technology, Shenzhen 518055, China*

[‡]*Department of Physics, South China University of Technology, Guangzhou 510640, China*

[¶]*Shenzhen Key Laboratory of Advanced Quantum Functional Materials and Devices and Department of Physics, Southern University of Science and Technology, China*

E-mail: scxbyang@scut.edu.cn; xuh@sustech.edu.cn

Abstract

The first metallic glass of Au-Si alloy has been discovered for over half a century, but its atomic structure is still puzzling. Herein, Au_8Si dodecahedrons with local five-fold symmetry are revealed as building blocks in Au-Si metallic glass, and the interconnection modes of Au_8Si dodecahedrons determine the medium-range order. With dimensionality reduction, the surface ordering is attributed to the motif transformation of Au_8Si dodecahedrons into planar Au_5Si pyramids with five-fold symmetry, and thus the self-assembly of Au_5Si pyramids leads to the formation of the ordered Au_2Si monolayer with the lowest energy. Furthermore, the structural similarity analysis is performed to unveil the physical origin of structural characteristics in different dimensions. The amorphism of Au-Si is due to the smooth energy landscape around the global minimum, while the ordered surface structure occurs due to the steep energy landscape.

Introduction

The Au-Si alloy was the first reported metallic glass, which was discovered in 1960 by rapid cooling.¹ Subsequently, bulk metallic glasses (BMGs) have attracted increasing attention due to their fundamental scientific interests and practical applications.²⁻⁴ Up to now, many computational methods and experimental techniques have been involved to investigate structures of BMGs.⁵⁻⁷ However, due to the absence of long-range order it remains challenging to determine atomic structures of BMGs.⁸ For example, a combination of experimental measurements and reverse Monte Carlo modelings failed to reproduce the precise packing structures of BMGs at the atomic level without sufficient structural information.⁹ Numerous structural models were proposed to improve the understanding of short-range order (SRO) in BMGs over the years,^{10,11} but these models are still difficult to figure out the medium-range order (MRO) of BMGs.¹² To overcome this challenge, the efficient cluster packing on a face-centered cubic lattice was proposed.¹³ In 2009, the MRO in BMGs was described by the packing mode of local motifs on a network with fractal dimension ($D_f = 2.32$),¹⁴ which is smaller than that of crystal ($D_f = 3.0$) or dodecahedron-quasicrystal ($D_f = 2.72$), indicating that filling the real space in these amorphous solids by building blocks is impossible. Therefore, unveiling the nature of atomic packing at the MRO scale in BMGs¹⁵ is a long-standing problem.

The Au-Si eutectic alloy has the extremely low eutectic temperature (359 °C) below the melting points of Au (1063 °C) and Si (1412 °C).¹⁶ At the lowest eutectic temperature, it has a composition of Au₈₂Si₁₈,¹⁶ which is the key to the catalytic growth of silicon nanowires¹⁷ because Si atoms maintain relatively high mobility at low temperatures.¹⁸ In recent years, although some theoretical studies reported possible alloy structures of Au-Si,¹⁹⁻²¹ the local ordering of Au-Si BMG is still lacking. Interestingly, two-dimensional (2D) crystallization was observed at the surface of Au-Si metallic glass,^{22,23} which has been experimentally confirmed to be an ordered rectangular structure²² with the proposed Si-Si bond on the surface. Shpyrko and co-workers²² claimed that the Au-Si surface ordering was induced

by surface-induced freezing,²⁴ but the ordered prefreezing surface will only appear near the transition temperature rather than a wide range of temperatures, inconsistent with the case of Au-Si. Moreover, density functional theory (DFT) calculations proved that the Si-Si bond is energetically unfavorable in the Au-Si alloy,^{18,20} implying the inconsistency in literature. This ordered surface plays a key role in crystal growth and solidification,^{25,26} but the atomic arrangement is still unclear. Therefore, uncovering the atomic structures of surface crystallization and Au-Si alloy will be beneficial for understanding exotic properties of Au-Si metallic glass.

In this article, *ab initio* molecular dynamics (AIMD) simulations were performed to investigate the bonding features of Au-Si in the undercooled state. The partial distribution function and coordination number analysis were employed to explore the SRO of liquid Au-Si alloy, and a set of Au₈Si dodecahedrons with local five-fold symmetry are the most energetically favorable motifs. The connection modes of different Au₈Si motifs with similar energies are substantial to reconstruct the Au-Si eutectic alloy, subtly affecting the structural stability of Au-Si. With dimensionality reduction, the basic building motifs, i.e., Au₈Si dodecahedrons, are reduced to be Au₅Si pyramids, which are Si-centered pentagons with five-fold symmetry. This phenomenon is confirmed by a systematic investigation of surface structures on the Au-Si alloy. Moreover, a 2D ordered Au₂Si monolayer composed of Au₅Si pyramids is found, which is more energetically favorable compared with all the earlier proposed surface structures. Notably, the simulated scanning tunneling microscope (STM) images are in much better agreement with the experimental results. Furthermore, the remarkable difference of structural similarity between the Au-Si bulk and surface structures is uncovered, providing insights into understanding why the bulk structure is a metallic glass while the surface alloy exhibits long-range order.

Results and discussion

To extract the inherent local SRO of $\text{Au}_{82}\text{Si}_{18}$, the initial configurations were constructed based on the Au bulk in thermal equilibrium, where a certain number of Au atoms were randomly replaced with Si atoms. To avoid the systematic error, 100 configurations were used to produce structural information, for instance, the average coordination numbers and the partial pair-correlation functions (see the details in the section of computational methods in the Supplemental Material (SM)[?]). As shown in Fig. 1(a), the partial pair-correlation functions $g_{ij}(r)$ of $\text{Au}_{82}\text{Si}_{18}$ were obtained after the undercooling process, where the simulation temperatures were quickly reduced to 300 K from 2000 K with a large cooling rate of 1×10^{11} K/s. The first peak of Au-Si is located at around 2.45 Å, suggesting the intensive mixing between Au and Si atoms. The first broad peak of Si-Si appears around 4 Å, showing that Si atoms are prohibited from being bonded together and surrounded by Au atoms. This phenomenon implies the existence of close packing that holds Si atoms like “solute” atoms in the center of polyhedrons. The coordination number (CN) analysis reveals that Au_8Si polyhedrons are the most frequent motifs in the Au-Si BMG, where the ratio reaches up to 79%, as shown in Fig. 1(b). It is worth noting that the frequent Au_8Si motifs have local five-fold symmetry in Fig. 1(c), which is responsible for the SRO. As a result, we can infer that the atomic structure of the Au-Si alloy is the self-assembly of Au_8Si dodecahedrons by connecting each other in a close-packed manner.

To determine the MRO in Au-Si, we need to reveal the origin of its structural stability, where the building blocks and connection rules are crucial to identify the local atomic ordering. According to the bonding features we obtained in Figs. 1(a), 1(b), we constructed a series of Au-Si configurations, which contain Au_nSi ($n = 6 - 10$) polyhedrons in a corner-sharing or edge-sharing mode, to explore stable structures of Au-Si alloy. As shown in Fig. 2(a), the Au_4Si structure has the lowest formation energy, which is in excellent agreement with the eutectic point of the Au-Si phase diagram.¹⁶ Particularly, two most stable structures with almost the same energy have been found, which are both comprised of Au_8Si

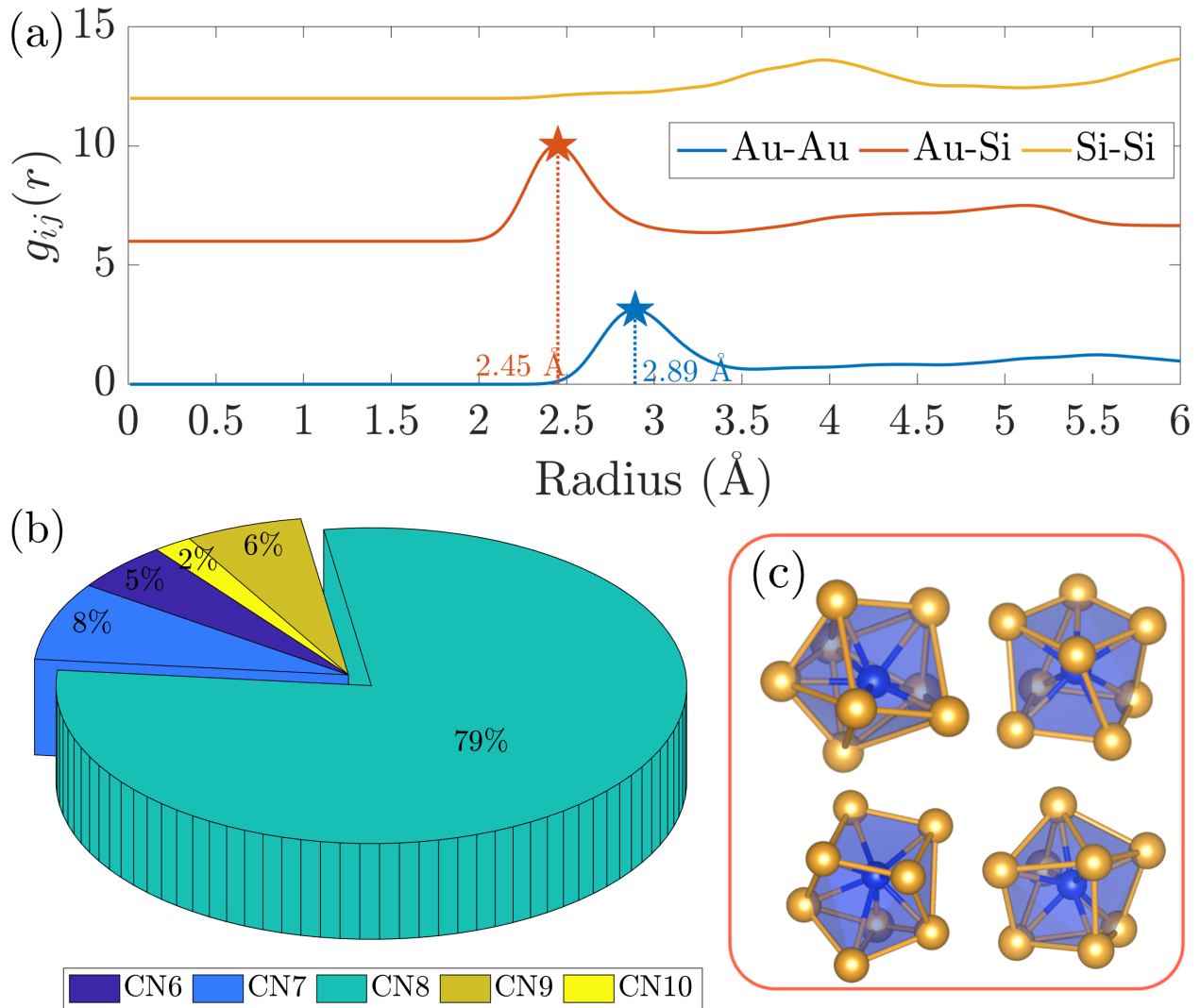


Figure 1: (a) The pair-correlation functions of $\text{Au}_{82}\text{Si}_{18}$ BMG at room temperature. For clarification, the Si-Si and Au-Si partials are shifted by 5 and 10, respectively. (b) The coordination number distribution of $\text{Au}_{82}\text{Si}_{18}$ BMG at room temperature. (c) The most frequent Au_8Si motifs in $\text{Au}_{82}\text{Si}_{18}$ BMG.

motifs in body-centered cubic (see Fig. 2(b)) and hexagonal close-packed (see Fig. 2(c)) structures. Moreover, we find that these two Au_8Si motifs can be combined together to form relatively stable structures with a larger number of atoms (see Fig. 2(d)), indicating that the connection modes are not dominant for the structural stability of Au-Si compared to the local atomic ordering. Therefore, the MRO at the atomic level is ascribed to the interconnection modes of Au_8Si motifs. It is worth noting that the formation energy distribution at Au concentration of 0.8 is very close, implying a flat energy landscape and the origin of

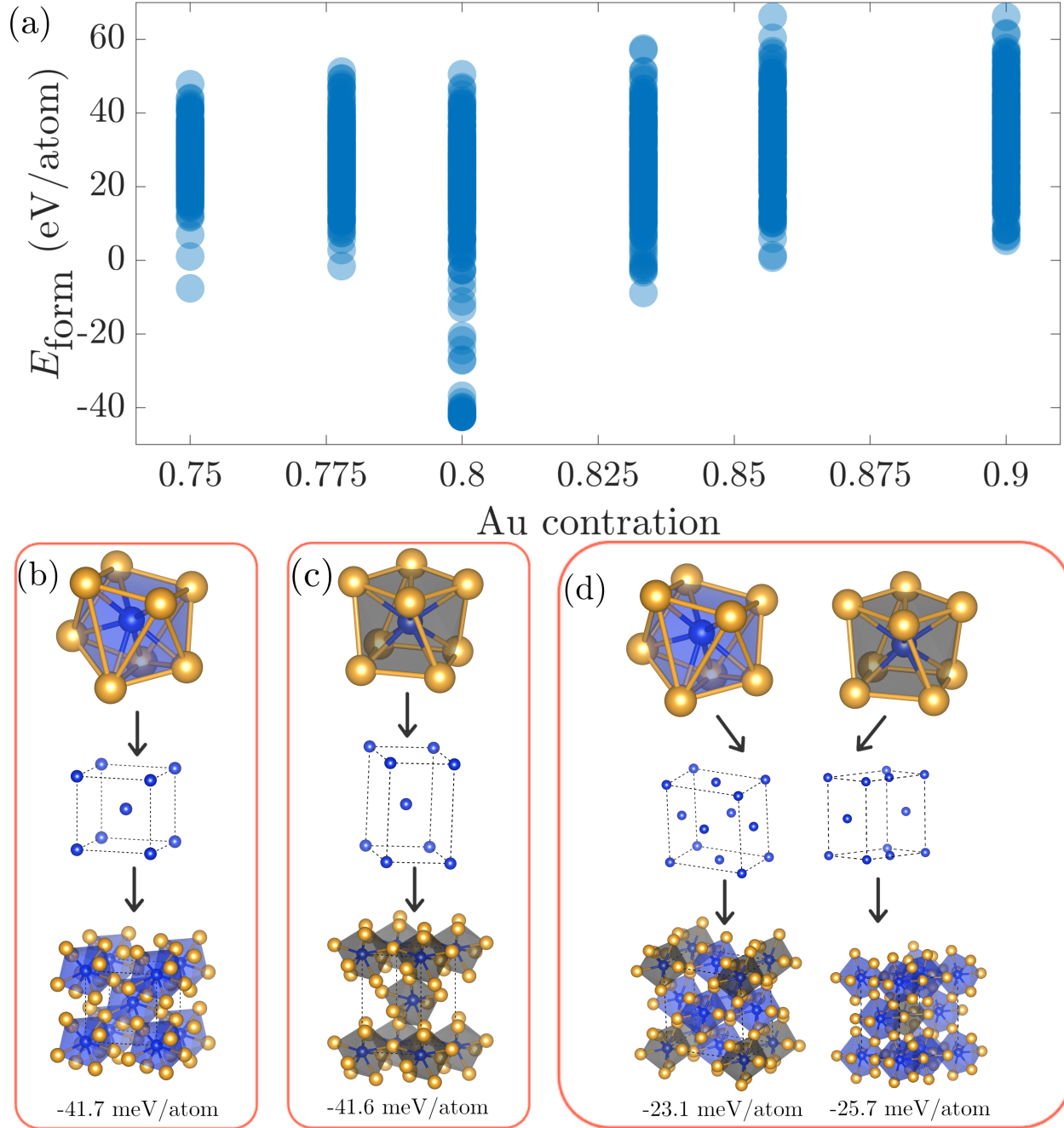


Figure 2: (a) The formation energy of Au-Si alloy with various Au concentrations. (b), (c) The most stable Au₄Si crystal structures, which are constructed by the fundamental Au₈Si motifs with different corner sharing modes. (d) The structure constructed from the two fundamental Au₈Si motifs with other corner sharing modes. Si and Au atoms are represented by blue and golden spheres, respectively.

formation mechanism in Au-Si.²⁷

The Au₈Si dodecahedrons with local five-fold symmetry are found to be the SRO in Au-

Si, but with dimensionality reduction the SRO of surface structures still leaves unknown. The surface crystallization of Au-Si BMG was observed in the last decade, however, the origin and atomic structure of the surface ordering are still in debate.^{22,24,26} We carried out AIMD simulations at 650 K to study the Si content in a roughly 25 Å-thick Au₈₂Si₁₈ slab with six layers, and five different slab models were considered to reduce systematic errors. During AIMD simulations Si atoms migrate to the surface from the central region, resulting in the higher concentration of Si atoms (around 42%) in the surface region, as shown in Fig. 3(a). Therefore, our results agree with the fact that Si atoms prefer the surface segregation in experiments,²² and the surface structure of Au-Si alloy is the mixture of Au and Si atoms.

Interestingly, this ordered rectangular surface structure with the same lattice parameters has also been experimentally observed by depositing Si atoms on the Au(111) substrate.^{28,29} Therefore, it is possible to search for the stable Au-Si surface structure on the Au(111) substrate. At the initial stage of the nucleation process, only one Si atom was introduced to react with the Au(111) substrate. The Au_nSi ($n = 3 - 7$) clusters with various coordination numbers for Si on Au(111) are shown in Fig. 3(b). It is apparent that the Au₅Si cluster with five-fold symmetry has the lowest formation energy, indicating that the Au₅Si pyramid is an energetically favorable motif in the Au-Si system.

To efficiently search for the possible structure of 2D Au-Si alloy, surface structure generation methods were employed to fertilize the structure database of Au-Si monolayers. We generated non-duplicated 2D Au-Si surface structures with various atomic ratios and distributions by the package of Structures of Alloy Generation And Recognition (SAGAR)^{30,31} and the crystal prediction algorithm RG2 based on space group theory and graph theory.³² To consider the lattice mismatch between monolayers and Au(111), we constructed various supercells. High-throughput first-principles calculations were performed to determine the possible surface structure on Au(111). As shown in Fig. S1 of the SM,[?] our results point out that Au-Si monolayers with Au₅Si pyramids are rather stable compared with those monolayers without Au₅Si pyramids, indicating that the Au₅Si motif with five-fold symmetry is

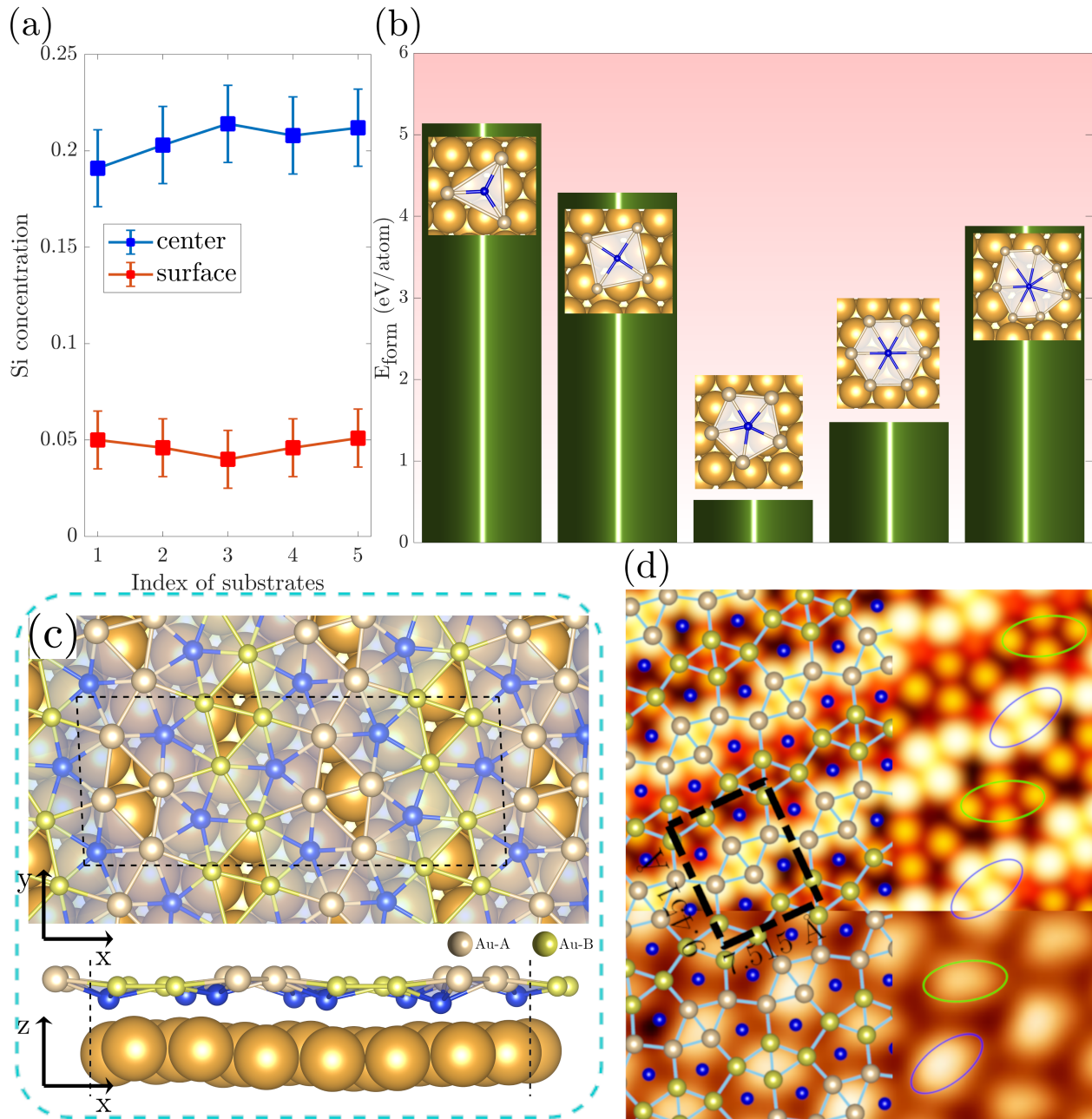


Figure 3: (a) The concentration of Si atoms in the surface layer and central region for five different slab models. (b) Formation energy of one Si atom on the Au(111) substrate. The insets show the corresponding structures. (c) The top view and side view of the stable slab model. Surface Si atoms are represented by blue spheres, and the black dashed lines mark the lattice of the slab. (d) The simulated (upper) and experimental (bottom) STM images. The experimental STM image is reprinted with permission from Ref.²⁹

the key SRO in surface structures of Au-Si.

Particularly, the most stable Au-Si monolayer on Au(111) is Au_2Si comprised of pen-

tagons and rhombuses, and the relaxed Au_2Si monolayer on $\text{Au}(111)$ are shown in Fig. 3(c). Intriguingly, the lattice parameters of the most stable Au_2Si monolayer are $a = 9.451 \text{ \AA}$ and $b = 7.515 \text{ \AA}$, which are in excellent agreement with previous experiment results.^{22,28,29} Si atoms are at a lower height than Au atoms in the Au-Si monolayer, implying that each rhombus contains four Au atoms in the topmost layer and Si atoms are separated by these Au_4 rhombuses. According to the experimental and simulated STM images shown in Fig. 3(d), the bright protrusions correspond to the Au_4 rhombuses. There are two types of protrusions in the Au_2Si monolayer that are rotated with respect to each other as highlighted by the ellipses,²⁸ corresponding to the two types of Au atoms with different heights in Fig. 3(c). The Au_5Si pyramids reflect dark pores in the STM image because the Si atoms are at a relatively low height. Therefore, we conclude that the Au_2Si monolayer forms by depositing Si atoms on the $\text{Au}(111)$ substrate.

To further confirm the existence of the ordered Au_2Si monolayer at the surface of $\text{Au}_{82}\text{Si}_{18}$ BMG, various Au-Si overlayers were deposited on the five slab models mentioned above in Fig. 3(a). The calculated formation energies on these five substrates are shown in Fig. S2 of the SM,[?] where the Au_2Si overlayer exhibits robust stability on different substrates, while other overlayers are less stable. This is strong evidence that the Au_2Si monolayer is the pretty stable ordered surface structure of Au-Si BMG.

The Au-Si BMG displays diverse structural characteristics in different dimensions, which is attributed to unusual Au-Si bonding properties and dimensionality reduction.²² To unveil the deep physical nature of the phenomenon, the energy landscape of the Au-Si system is comprehensively investigated to uncover the origin of the distinction between bulk and surface. If the global minimum is surrounded by numerous local minima, namely, lots of low energy saddle points are around the ground state structure, this system is a glassy system, otherwise, it belongs to a structure seeker system.²⁷ For instance, the carbon and boron nitride systems can be clearly identified as structure seekers while the large boron cluster systems are glassy.³³

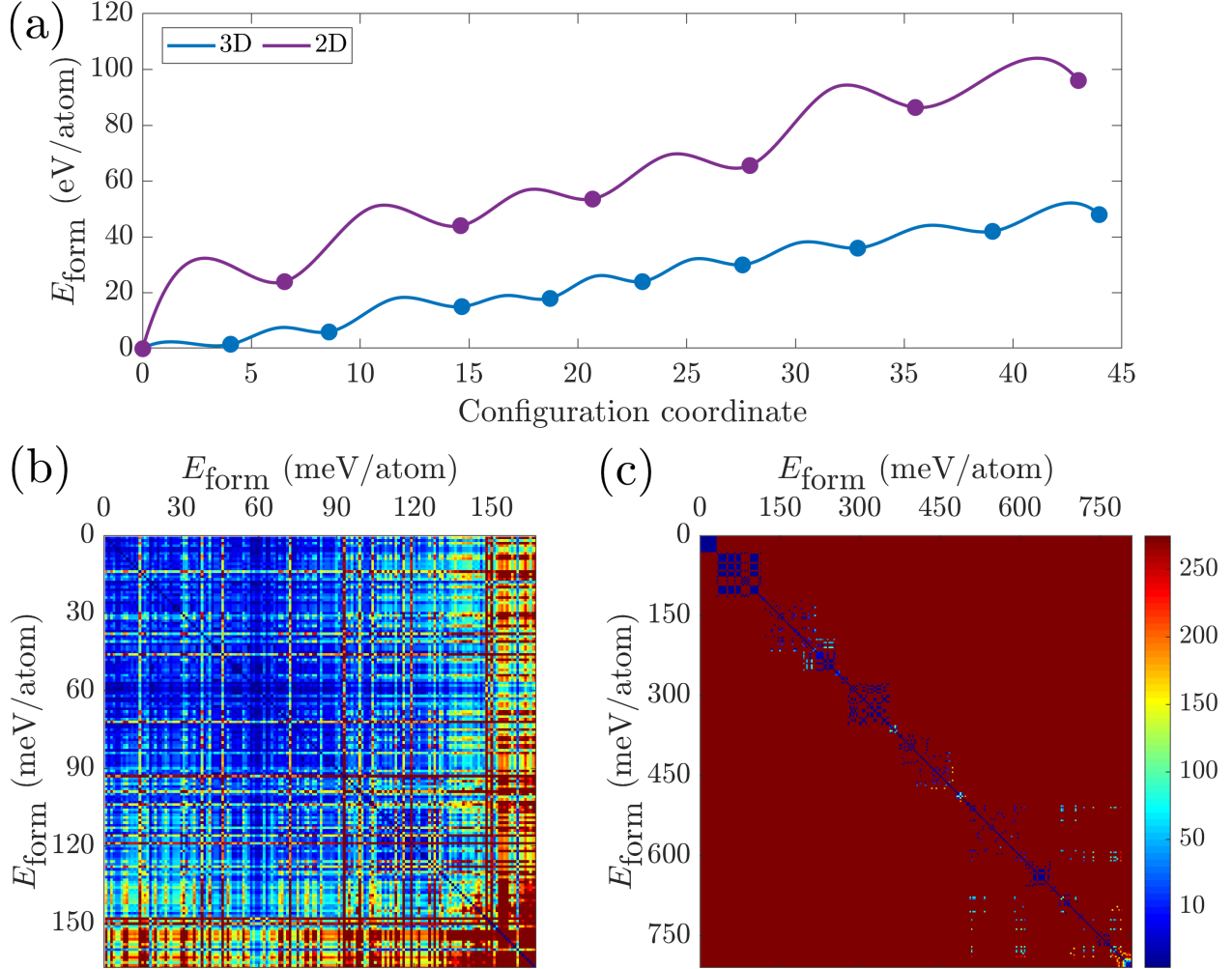


Figure 4: (a) The distance-energy analysis for low-energy Au-Si structures in 2D and 3D systems. The structural similarity distribution in bulk and surface Au-Si are shown in (b) and (c), respectively. The colors represent the similarity degree between two structures, where blue/red represents the small/large distance, corresponding to the shared colorbar in the right, which is applicable for both 3D and 2D systems.

To define the distance between any two structures, we employed the Smooth Overlap of Atomic Positions (SOAP) descriptor³⁴ to encode regions of atomic geometries by using local expansion of a gaussian smeared atomic density. The bulk Au-Si alloy and surface structures were generated by SAGAR and RG2 algorithm as mentioned above. We chose several low-energy Au-Si structures to perform the distance-energy analysis³⁵ in 2D and three-dimensional (3D) systems as shown in Fig. 4(a). For 2D surface structures, the formation energy increases rather quickly with configuration coordinate, and the saddle

points are relatively far away from each other according to the configuration coordinate compared to the case of 3D bulk structures. In the bulk case, the blue color in Fig. 4(b) represents that the distances among the low energy structures are rather small, indicating that there is a low energy barrier between two local minima. This feature leads to the fact that it is difficult to form any ordered bulk Au-Si alloy during the rapid cooling process, which is confirmed by molecular dynamics simulations in Au-Si BMG.³⁶ However, the image of the Au-Si surface structure (see Fig. 4(c)) is almost filled with red color, implying that distances are much larger between low and high energy structures. Therefore, the long-range ordering can easily appear in surface structures.

In summary, we have uncovered the local ordering of Au-Si, where the Au_8Si motifs with local five-fold symmetry are the basic building blocks and the different connection modes reveal the MRO. With dimensionality reduction, the SRO of Au-Si surface structure has been transformed into Au_5Si pyramids with five-fold symmetry. We have concluded that the Au_2Si monolayer composed of Au_5Si pyramids is the surface structure observed in experiments, due to the lowest formation energy and excellent agreement with STM images. Employing the structural similarity matrix based on the SOAP descriptor to metricize the distance among Au-Si structures, we have shown that there is a smooth energy landscape with dense local minima for the Au-Si bulk, while the energy landscape of Au-Si surface structures is relatively steep around the ground state. Our work not only supplies a structure search method to determine the Au-Si structures in different dimensions but also expounds on the intrinsic origin of the order-disorder transition in Au-Si alloy from 2D to 3D, which may pave a promising avenue to explore the novel properties in other metallic glasses.

Acknowledgement

This work was supported by the Science, Technology, and Innovation Commission of Shenzhen Municipality (Grant Nos. RCYX20200714114523069 and ZDSYS20190902092905285),

the National Natural Science Foundation of China (No. 11974160), and Key-Area Research and Development Program of Guangdong Province (No. 2020B010183001). The computer time at the Center for Computational Science and Engineering at Southern University of Science and Technology is gratefully acknowledged.

References

- (1) Klement, W.; Willens, R. H.; Duwez, P. Non-crystalline Structure in Solidified Gold–Silicon Alloys. *Nature* **1960**, *187*, 869–870.
- (2) Fujita, T.; Konno, K.; Zhang, W.; Ku, V.; Matsuura, M.; Inoue, A.; Sakurai, T.; Chen, M. W. Atomic-Scale Heterogeneity of a Multicomponent Bulk Metallic Glass with Excellent Glass Forming Ability. *Phys. Rev. Lett.* **2009**, *103*, 075502.
- (3) Inoue, A. Stabilization of metallic supercooled liquid and bulk amorphous alloys. *Acta Mater.* **2000**, *48*, 279–306.
- (4) Hirata, A.; Kang, L. J.; Fujita, T.; Klumov, B.; Matsue, K.; Kotani, M.; Yavari, A. R.; Chen, M. W. Geometric Frustration of Icosahedron in Metallic Glasses. *Science* **2013**, *341*, 376–379.
- (5) Kelton, K. F.; Lee, G. W.; Gangopadhyay, A. K.; Hyers, R. W.; Rathz, T. J.; Rogers, J. R.; Robinson, M. B.; Robinson, D. S. First X-Ray Scattering Studies on Electrostatically Levitated Metallic Liquids: Demonstrated Influence of Local Icosahedral Order on the Nucleation Barrier. *Phys. Rev. Lett.* **2003**, *90*, 195504.
- (6) Hirata, A.; Guan, P.; Fujita, T.; Hirotsu, Y.; Inoue, A.; Yavari, A. R.; Sakurai, T.; Chen, M. Direct observation of local atomic order in a metallic glass. *Nat. Mater.* **2011**, *10*, 28–33.

- (7) Zhong, L.; Wang, J.; Sheng, H.; Zhang, Z.; Mao, S. X. Formation of monatomic metallic glasses through ultrafast liquid quenching. *Nature* **2014**, *512*, 177–180.
- (8) Cheng, Y. Q.; Ma, E.; Sheng, H. W. Atomic Level Structure in Multicomponent Bulk Metallic Glass. *Phys. Rev. Lett.* **2009**, *102*, 245501.
- (9) Keen, D. A.; McGreevy, R. L. Structural modelling of glasses using reverse Monte Carlo simulation. *Nature* **1990**, *344*, 423–425.
- (10) BERNAL, J. D. Geometry of the Structure of Monatomic Liquids. *Nature* **1960**, *185*, 68–70.
- (11) GASKELL, P. H. A new structural model for transition metal–metalloid glasses. *Nature* **1978**, *276*, 484–485.
- (12) Sheng, H. W.; Luo, W. K.; Alamgir, F. M.; Bai, J. M.; Ma, E. Atomic packing and short-to-medium-range order in metallic glasses. *Nature* **2006**, *439*, 419–425.
- (13) Miracle, D. B. A structural model for metallic glasses. *Nat. Mater.* **2004**, *3*, 697–702.
- (14) Ma, D.; Stoica, A. D.; Wang, X.-L. Power-law scaling and fractal nature of medium-range order in metallic glasses. *Nat. Mater.* **2009**, *8*, 30–34.
- (15) Miracle, D. B.; Egami, T.; Flores, K. M.; Kelton, K. F. Structural Aspects of Metallic Glasses. *MRS Bull.* **2007**, *32*, 629–634.
- (16) Okamoto, H.; Massalski, T. B. The Au-Si (Gold-Silicon) system. *Bull. Alloy Phase Diagrams* **1983**, *4*, 190–198.
- (17) Hannon, J. B.; Kodambaka, S.; Ross, F. M.; Tromp, R. M. The influence of the surface migration of gold on the growth of silicon nanowires. *Nature* **2006**, *440*, 69–71.

- (18) Pasturel, A.; Tasci, E. S.; Sluiter, c. H. F.; Jakse, N. Structural and dynamic evolution in liquid Au-Si eutectic alloy by ab initio molecular dynamics. *Phys. Rev. B* **2010**, *81*, 140202.
- (19) Tasci, E. S.; cel H.F. Sluiter,; Pasturel, A.; Villars, P. Liquid structure as a guide for phase stability in the solid state: Discovery of a stable compound in the Au-Si alloy system. *Acta Mater.* **2010**, *58*, 449–456.
- (20) Dong, Y.-H.; Lu, W.-C.; Xu, X.; Zhao, X.; Ho, K. M.; Wang, C. Z. Theoretical search for possible Au-Si crystal structures using a genetic algorithm. *Phys. Rev. B* **2017**, *95*, 134109.
- (21) Lee, S.-H.; Hwang, G. S. Structure, energetics, and bonding of amorphous Au-Si alloys. *J. Chem. Phys.* **2007**, *127*, 224710.
- (22) Shpyrko, O. G.; Streitl, R.; Balagurusamy, V. S. K.; Grigoriev, A. Y.; Deutsch, M.; Ocko, B. M.; Meron, M.; Lin, B.; Pershan, P. S. Surface Crystallization in a Liquid AuSi Alloy. *Science* **2006**, *313*, 77–80.
- (23) Kurtuldu, G.; Löffler, J. F. Multistep Crystallization and Melting Pathways in the Free-Energy Landscape of a Au-Si Eutectic Alloy. *Adv. Sci.* **2020**, *7*, 1903544.
- (24) Pluis, B.; Frenkel, D.; van der Veen, J. Surface-induced melting and freezing II. A semi-empirical Landau-type model. *Surf. Sci.* **1990**, *239*, 282–300.
- (25) Chatterjee, D.; Annamareddy, A.; Ketkaew, J.; Schroers, J.; Morgan, D.; Voyles, P. M. Fast Surface Dynamics on a Metallic Glass Nanowire. *ACS Nano* **2021**, *15*, 11309–11316.
- (26) Panciera, F.; Tersoff, J.; Gamalski, A. D.; Reuter, k. C.; Zakharov, D.; Stach, E. A.; Hofmann, S.; Ross, F. M. Surface Crystallization of Liquid Au-Si and Its Impact on Catalysis. *Adv. Mater.* **2019**, *31*, 1806544.

- (27) De, S.; Schaefer, B.; Sadeghi, A.; Sicher, M.; Kanhere, D. G.; Goedecker, S. Relation between the Dynamics of Glassy Clusters and Characteristic Features of their Energy Landscape. *Phys. Rev. Lett.* **2014**, *112*, 083401.
- (28) Sadeddine, S.; Enriquez, H.; Bendounan, A.; Ku Das, P.; Vobornik, I.; Kara, A.; ne, A. J.; Sirotti, F.; Dujardin, G.; Oughaddou, H. Compelling experimental evidence of a Dirac cone in the electronic structure of a 2D Silicon layer. *Sci. Rep.* **2017**, *7*, 44400.
- (29) Stpniak-Dybala, A.; Dyniec, P.; Kopciuszyski, e.; Zdyb, R.; Jałochowski, M.; Krawiec, i. Planar Silicene: A New Silicon Allotrope Epitaxially Grown by Segregation. *Adv. Funct. Mater.* **2019**, *29*, 1906053.
- (30) He, C.-C.; Qiu, S.-B.; Yu, J.-S.; Liao, J.-H.; Zhao, Y.; Yang, X.-B. Atom Classification Model for Total Energy Evaluation of Two-Dimensional Multicomponent Materials. *J. Phys. Chem. A* **2020**, *124*, 4506–4511.
- (31) He, C.-C.; Liao, J.-H.; Qiu, S.-B.; Yu-Zhao,; Yang, X.-B. Biased screening for multi-component materials with Structures of Alloy Generation And Recognition (SAGAR). *Comput. Mater. Sci.* **2021**, *193*, 110386.
- (32) Shi, X.; He, C.; Pickard, C. J.; Tang, C.; Zhong, J. Stochastic generation of complex crystal structures combining group and graph theory with application to carbon. *Phys. Rev. B* **2018**, *97*, 014104.
- (33) De, S.; Willand, A.; Amsler, M.; Pochet, P.; Genovese, L.; Goedecker, S. Energy Landscape of Fullerene Materials: A Comparison of Boron to Boron Nitride and Carbon. *Phys. Rev. Lett.* **2011**, *106*, 225502.
- (34) Bartók, A. P.; Kondor, R.; Csányi, G. On representing chemical environments. *Phys. Rev. B* **2013**, *87*, 184115.

- (35) Sadeghi, A.; Ghasemi, S. A.; Schaefer, B.; Mohr, S.; Lill, k. A.; Goedecker, S. Metrics for measuring distances in configuration spaces. *J. Chem. Phys.* **2013**, *139*, 184118.
- (36) Ran, C.-Y.; Zhou, L.-L.; Liang, Y.-C.; Mo, Y.-F.; Chen, Q.; Tian, Z.-A.; Liu, R.-S.; Gao, T.-H.; Xie, Q. Study on Si-like and topologically close-packed structures during rapid solidification of Au-Si alloys. *J. Non-Cryst. Solids* **2021**, *563*, 120787.

Graphical TOC Entry

